DISCRIMINATION REPORT

ESTCP PROJECT # MM-0437

REV. 1

SITE LOCATION:
FE WARREN AFB, CHEYENNE, WY

DEMONSTRATOR:
LAWRENCE BERKELEY NATIONAL LABORATORY
ONE CYCLOTRON ROAD, MS: 90R1116
BERKELEY, CA 94720
p.o.c. Erika Gasperikova, egasperikova@lbl.gov, 510-486-4930

TECHNOLOGY TYPE/PLATFORM:
BUD/CART

OCTOBER 2008

Disclaimer

Acknowledgment

This work was supported by Work For Others funding from Berkeley Lab, provided by the Director, Office of Science, of the U.S. Department of Energy under Contract No. DE-AC02-05CH11231.

TABLE OF CONTENTS

1. INTRODUCTION 5

1.1 BACKGROUND 5
1.2 OBJECTIVE OF THE DEMONSTRATION 6

2. TECHNOLOGY DESCRIPTION 6

2.1 TECHNOLOGY DEVELOPMENT AND APPLICATION 6
2.2 PREVIOUS TESTING OF THE TECHNOLOGY 14
2.3 ADVANTAGES AND LIMITATIONS OF THE TECHNOLOGY 14

3. DEMONSTRATION DESIGN 15

3.1 OPERATIONAL PARAMETERS FOR THE TECHNOLOGY 15
3.2 PERIOD OF OPERATION 18

4. DATA ANALYSIS AND INTERPRETATION 19

5. PERFORMANCE ASSESSMENT 31

6. COST ASSESSMENT 34

7. REFERENCES 35

APPENDIX 1. UXO DISCRIMINATION USING TRAINING DATA 38

LIST OF FIGURES

FIGURE 1. BERKELEY UXO DISCRIMINATOR (BUD) 7
FIGURE 2. INVERSION RESULTS FOR THE PRINCIPAL POLARIZABILITIES, LOCATION AND ORIENTATION OF 81 MM PROJECTILE 9
FIGURE 3. INVERSION RESULTS FOR THE PRINCIPAL POLARIZABILITIES, LOCATION AND ORIENTATION OF 105 MM PROJECTILE 10
FIGURE 4. INVERSION RESULTS FOR THE PRINCIPAL POLARIZABILITIES, LOCATION AND ORIENTATION OF 19X8 CM SCRAP METAL 10
FIGURE 5. 10% UNCERTAINTY IN LOCATION AS A FUNCTION OF OBJECT DIAMETER AND DEPTH OF THE DETECTION FOR BUD WITH RECEIVERS 0.2 M ABOVE THE GROUND 11
FIGURE 6. 10% UNCERTAINTY IN LOCATION AS A FUNCTION OF OBJECT DIAMETER AND DEPTH OF THE DISCRIMINATION FOR BUD WITH RECEIVERS 0.2 M ABOVE THE GROUND..... 12
FIGURE 7. PRINCIPAL POLARIZABILITY CURVES AS A FUNCTION OF TIME FOR 75 MM PROJECTILE. 16
FIGURE 8. BUD GPO DETECTION MAP. 21
FIGURE 9. PRINCIPAL POLARIZABILITY CURVES AS A FUNCTION OF TIME FOR 37 MM PROJECTILE. 22
FIGURE 10. PRINCIPAL POLARIZABILITY CURVES AS A FUNCTION OF TIME FOR A HAND GRENADE, MK II..... 22
FIGURE 11. PRINCIPAL POLARIZABILITY CURVES AS A FUNCTION OF TIME FOR 60 MM MORTAR.... 23
FIGURE 12. PRINCIPAL POLARIZABILITY CURVES AS A FUNCTION OF TIME FOR 3" STOKES MORTAR. 23
FIGURE 13. PRINCIPAL POLARIZABILITY CURVES AS A FUNCTION OF TIME FOR 75 MM AP PROJECTILE. 24
FIGURE 14. PRINCIPAL POLARIZABILITY CURVES AS A FUNCTION OF TIME FOR 81 MM MORTAR.... 24
FIGURE 15. PRINCIPAL POLARIZABILITY CURVES AS A FUNCTION OF TIME FOR 2.36" ROCKET. 25
FIGURE 16. PRINCIPAL POLARIZABILITY CURVES AS A FUNCTION OF TIME FOR SCRAP METAL..... 26
FIGURE 17. BUD DETECTION MAP OF THE PRIORITY 1 AREA. 27
FIGURE 18. PROBABILITY OF A METALLIC OBJECT BEING A SINGLE UXO. VALUES ARE GIVEN IN FRACTIONS (1=100%, 0.1=10%) 30
FIGURE 19. PRIORITY DIG MAP –GREEN DOTS ARE IDENTIFIED AS SCRAP WHILE RED DOTS ARE LOCATIONS THAT NEED TO BE DUG. 31
FIGURE 20: ESTIMATED ROC CURVE FOR THE TARGETS PRIORITY DIG LIST. 34

LIST OF TABLES

TABLE 1. TOTAL TIME OF MAJOR DEMONSTRATION ACTIVITIES 18

ACRONYMS

AEM	Active Electromagnetic System
AFB	Air Force Base
BUD	Berkeley UXO Discriminator
ESTCP	Environmental Security Technology Certification Program
FPGA	Field Programmable Gate Array
GPO	Geophysical Prove Out
GPS	Global Positioning System
LBNL	Lawrence Berkeley National Laboratory
RTK	Real Time Kinematic
QA/QC	Quality Assurance/Quality Control
SERDP	Strategic Environmental Research and Development Program
UXO	Unexploded Ordnance
YPG	Yuma Proving Ground

1. INTRODUCTION

1.1 Background

The FY06 Defense Appropriation contains funding for the "Development of Advanced, Sophisticated, and Discrimination Technologies for UXO Cleanup" in the Environmental Security Technology Certification Program. In 2003, the Defense Science Board observed: "The … problem is that instruments that can detect the buried UXOs also detect numerous scrap metal objects and other artifacts, which leads to an enormous amount of expensive digging. Typically 100 holes may be dug before a real UXO is unearthed! The Task Force assessment is that much of this wasteful digging can be eliminated by the use of more advanced technology instruments that exploit modern digital processing and advanced multi-mode sensors to achieve an improved level of discrimination of scrap from UXOs."

Significant progress has been made in discrimination technology. To date, testing of these approaches has been primarily limited to test sites with only limited application at live sites. Acceptance of discrimination technologies requires demonstration of system capabilities at UXO sites under real world conditions. FE Warren Air Force Base (AFB) in Cheyenne, WY is one such site.

1.2 Objective of the Demonstration

The demonstration objective was to determine the discrimination capabilities, cost and reliability of the Berkeley UXO Discriminator (BUD) in discrimination of UXO from scrap metal in real life conditions. Lawrence Berkeley National Laboratory performed a detection and discrimination survey of the Priority 1 area (~ 5 acres) of the FE Warren AFB. The data included a system characterization with the emplaced calibration items and targets in the Geophysical Prove Out (GPO) area.

2. TECHNOLOGY DESCRIPTION

2.1 Technology Development and Application

The Environmental Security Technology Certification Program, ESTCP, has supported Lawrence Berkeley National Laboratory (LBNL) in the development of the Berkeley UXO Discriminator (BUD) that not only detects the object itself but also quantitatively determines its size, shape, and orientation. Furthermore, BUD performs target characterization from a single position of the sensor platform above a target. BUD was designed to detect UXO in the 20 mm to 155 mm size range for depths between 0 and 1.5 m, and to characterize them in a depth range from 0 to 1.1 m. The system incorporates three orthogonal transmitters, and eight pairs of differenced receivers. The transmitter-receiver assembly together with the acquisition box, as well as the battery power and global positioning system (GPS) receiver, is mounted on a small

cart to assure system mobility. System positioning is provided by a state-of-the-art Real Time Kinematic (RTK) GPS receiver. The survey data acquired by BUD is processed by software developed by LBNL, which is efficient and simple, and can be operated by relatively untrained personnel. BUD is shown in Figure 1.

Figure 1. Berkeley UXO Discriminator (BUD)

Eight receiver coils are placed horizontally along the two diagonals of the upper and lower planes of the two horizontal transmitter loops. These receiver coil pairs are located on symmetry lines through the center of the system and each pair sees identical fields during the on-time of current pulses in the transmitter coils. They are wired in opposition to produce zero output during the on–time of the pulses in three orthogonal transmitters. Moreover, this configuration

dramatically reduces noise in measurements by canceling background electromagnetic fields (these fields are uniform over the scale of the receiver array and are consequently nulled by the differencing operation), and by canceling noise contributed by the tilt of the receivers in the Earth's magnetic field, and greatly enhances the receivers sensitivity to gradients of the target response.

Data acquisition is performed on a single board. The transmitter coils are powered by circuits which are separate from the data acquisition board. These pulsers provide resonant circuit switching to create bi-polar half-sine pulses of 350 μs width. The current peaks at 18 A which results in a resonant receiver circuit voltage of ~750 Volts. The operational overall half-sine duty cycle is ~12%. The resonant frequency of the inductive load is ~90 kHz. Transients are digitized with a sampling interval of 4 μs. The sensors are critically damped 6-inch 325 turn loops with a self-resonant frequency of 25 kHz. The data acquisition board has 12 high-speed ADC channels. Eight of these channels are used for the signal from receiver coils, and the remaining four channels provide information about the system (i.e. tilt information, odometer).

It has been demonstrated that a satisfactory classification scheme is one that determines the principal dipole polarizabilities of a target – a near intact UXO displays a single major polarizability coincident with the long axis of the object and two equal transverse polarizabilities. The induced moment of a target depends on the strength of the transmitted inducing field. The moment normalized by the inducing field is the polarizability. This description of the inherent polarizabilities of a target constitutes a major advance in discriminating UXO from irregular

scrap metal. Figures 2-4 illustrate the discrimination capability of the system for UXO objects (Figures 2 and 3), and scrap metal (Figure 4). All three figures have estimated principal polarizabilities as a function of time plotted on the left, values of true and estimated location and orientation on the right, and object images at the bottom. While UXO objects have a single major polarizability coincident with the long axis of the object and two equal transverse polarizabilities (Figure 2-3), the scrap metal exhibits three distinct principal polarizabilities (Figure 4). The locations and orientations are recovered within a few percent of true values for all three objects.

These results clearly show that a multiple transmitter – multiple receiver system can resolve the intrinsic polarizabilities of a target and that there are very clear distinctions between symmetric intact UXO and irregular scrap metal.

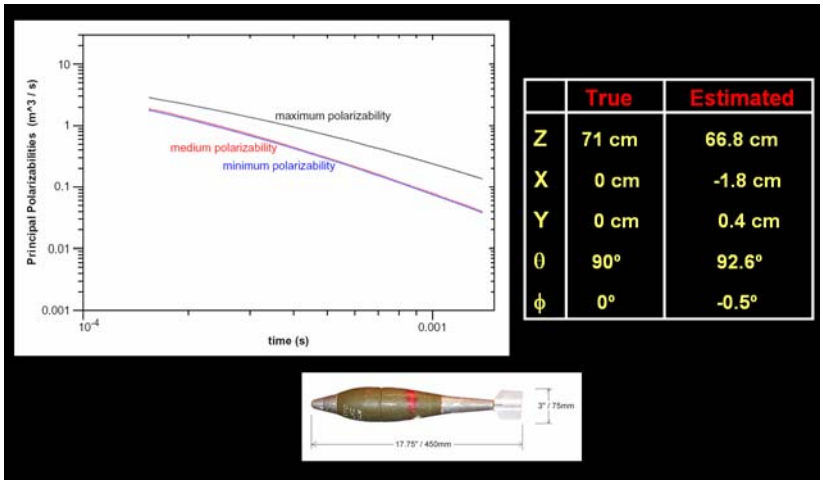

Figure 2. Inversion results for the principal polarizabilities, location and orientation of 81 mm projectile

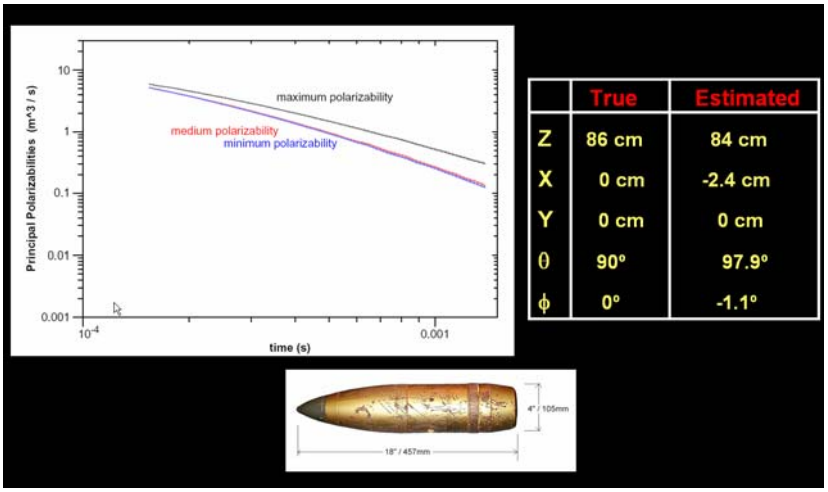

Figure 3. Inversion results for the principal polarizabilities, location and orientation of 105 mm projectile

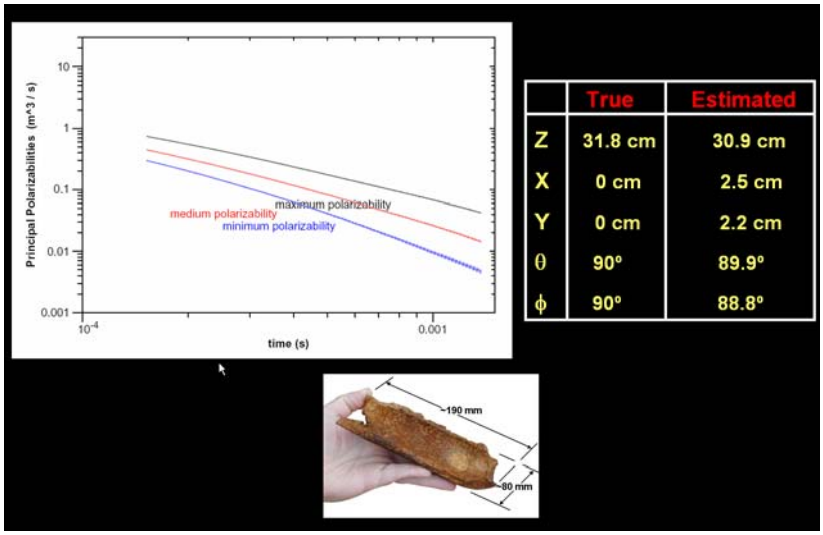

Figure 4. Inversion results for the principal polarizabilities, location and orientation of 19x8 cm scrap metal

The detection performance of the system is governed by a size-depth curve shown in Figure 5. This curve was calculated for BUD assuming that the receiver plane is 0.2 m above the ground. Figure 5 shows that, for example, BUD can detect an object with 0.1 m diameter down to the

depth of 0.9 m with depth uncertainty of 10%. Any objects buried at a depth of more than 1.3 m will have a low probability of detection. The discrimination performance of the system is governed by a size-depth curve shown in Figure 6. Again, this curve was calculated for BUD assuming that the receiver plane is 0.2 m above the ground. Figure 6 shows that, for example, BUD can discriminate an object with 0.1 m diameter down to the depth of 0.63 m with depth uncertainty of 10%. Any objects buried at the depth more than 0.9 m will have a low probability of discrimination.

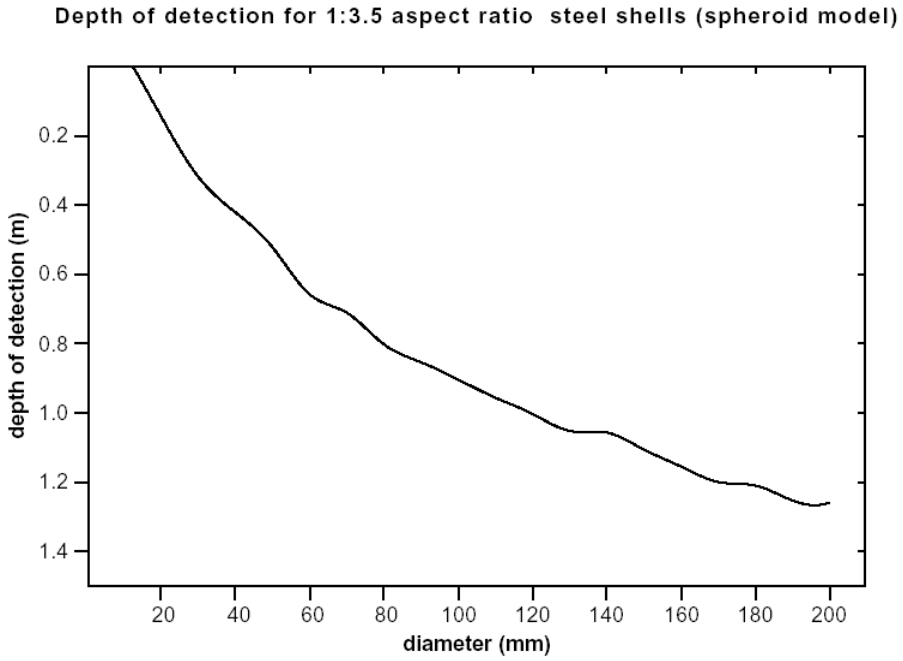

Figure 5. 10% uncertainty in location as a function of object diameter and depth of the detection for BUD with receivers 0.2 m above the ground

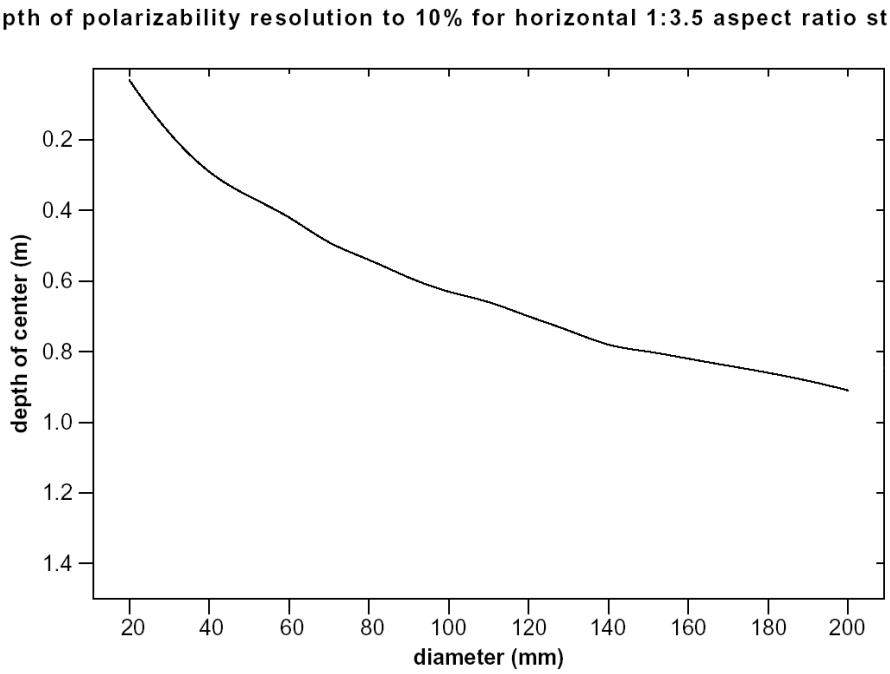

Figure 6. 10% uncertainty in polarizability as a function of object diameter and depth of the discrimination for BUD with receivers 0.2 m above the ground

Object orientation estimates and equivalent dipole polarizability estimates used for large and shallow UXO/scrap discrimination are more problematic as they are affected by higher order (non-dipole) terms induced in objects due to source field gradients along the length of the objects. For example, a vertical 0.4 m object directly below the system needs to be about 0.90 m deep for perturbations due to gradients along the length of the object to be of the order of 20 % of the uniform field object response. Similarly, vertical objects 0.5 m, and 0.6 m long need to be 1.15 m, and 1.42 m, respectively, below the system. For horizontal objects the effect of gradients across the objects' diameter are much smaller. For example, 155 mm and 105 mm projectiles need to be only 0.30 m, and 0.19 m, respectively, below the system. A polarizability index (in cm^3), which is an average value of the product of time (in seconds) and polarizability

rate (in m^3/s) over the 34 sample times logarithmically spaced from 140 to 1400 μs, and three polarizabilities, can be calculated for any object. We use this polarizability index to decide when the object is in a uniform source field. Objects with the polarizability index smaller than 600 cm^3 and deeper than 1.8 m below BUD, or smaller than 200 cm^3 and deeper than 1.35 m, or smaller than 80 cm^3 and deeper than 0.90 m, or smaller than 9 cm^3 and deeper than 0.20 m below BUD are sufficiently deep that the effects of vertical source field gradients should be less than 15%. All other objects are considered large and shallow objects.

To assure proper object identification and UXO/scrap discrimination, in the case of large and shallow objects, we take measurements at five sites spaced 0.5 m along a line traversing the object. Initially, object orientation is estimated from the response at the most distant of these sites. Then, the site, for which the line from the object center to the BUD bottom receiver plane center that is closest to being 90° to the orientation of the objects' interpreted axis of greatest polarizability, is selected. The data from this site have the smallest source field gradients in the direction of the estimated axis of greatest polarizability. The results of polarizability inversion from this site is used for object classification.

At FE Warren AFB the range of UXO targets goes from 37 mm projectile up to 81 mm mortar. The BUD detection threshold is based on the signal strength relative to levels of background response variation observed at Yuma Proving Ground. Measured signal strengths (field value) normalized by this background variation for a 37 mm projectile at 40 cm depth (the depth equal to 11 x diameter) at our Richmond field test facility were around 15, therefore the detection threshold is set to 7, which is 50% of that value.

2.2 Previous Testing of the Technology

The performance of the BUD has been demonstrated at a local test site in California, as well as at the Yuma Proving Ground (YPG), Arizona, and Camp Sibert, Alabama. The results have been presented at various meetings and published in scientific journals.

2.3 Advantages and Limitations of the Technology

This is the first AEM system that can not only detect UXO but also discriminate it from non-UXO/scrap and give its characteristics (location, size, polarizability). Moreover, the object can be characterized from a single position of the sensor platform above the object. BUD was designed to detect UXO in the 20 mm to 155 mm size range buried anywhere from the surface down to 1.5 m depth. Any objects buried at the depth more than 1.5 m will have a low probability of detection. In addition, BUD was designed to characterize UXO in the same size range in depths between 0 and 1.1 m. Any objects buried at the depth more than 1.1 m will have a low probability of discrimination. With existing algorithms in the system computer it is not possible to recover the principal polarizabilities of large objects close to the system. Detection of large shallow objects is assured, but at present discrimination is not. Post processing of the field data is required for shape discrimination of large shallow targets. See Chapter 2.1 for details.

3. DEMONSTRATION DESIGN

3.1 Operational Parameters for the Technology

We shipped all the equipment and supplies to the test site using a container and a commercial trucking company. Personnel flew and drove to the site in rented vehicles. Equipment was stored in the shipping container which was dropped off close to the survey area. The survey was contracted out to a geophysical survey company Zapata Engineering. The survey team consisted of two people, and a PI and additional LBL employee at the beginning of the survey who provided a field crew training. Data quality control and progress was done remotely. The field crew uploaded acquired data on the LBNL server daily, and if there were some problems after reviewing the data the field crew was instructed to repeat some measurements.

Assembling the cart, connecting the batteries, checking the data acquisition system and verifying the data records took about 30 minutes every morning. This was followed by system calibration using 75 mm projectile. This point was measured every morning and every evening. Responses of the calibration target were consistent and repeatable throughout the survey. The principal polarizability curves as a function of time for our calibration target are shown in Figure 7.

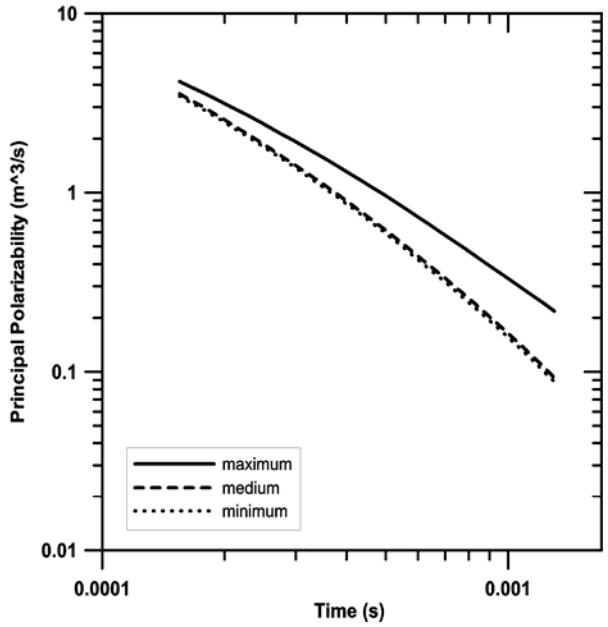

Figure 7. Principal polarizability curves as a function of time for 75 mm projectile.

The primary mode of BUD operation was simultaneous detection and characterization/ discrimination, although due to a time and weather constrains we used the cued mode in one part of the GPO area. The Priority 1 survey area was divided into two hundred ~100-m long lines in a more-less east-west direction. Line spacing in the orthogonal direction (north-south) was 1 m. We surveyed lines using a GPS and strings and then sprayed them in with a biodegradable paint. BUD was pushed along the line at a constant speed in a search mode. Data were recorded and stored continuously. In principle, any object within the 1 m × 1 m footprint of the horizontal transmitter coil and 1.2 m in front of the system can be detected and characterized. The detection threshold was set to 7. In the search mode the operator was alerted to the presence of a target every time the signal level exceeded the detection threshold. The threshold value was recorded together will data file name, acquisition time, and BUD GPS location. If the target was inside of the BUD footprint, the operator stopped and a full sequence of measurements was

initiated. The three discriminating polarizability responses were recorded and visually presented on the computer screen. The depth and horizontal location with respect to the cart were recorded, together with the GPS location of the reference point on the cart. Then the cart again moved at a constant speed in search mode until the next target was detected and the discrimination process was repeated. This mode of operation has the advantage that target reacquisition is not necessary for characterization. As described in Chapter 2.1, object orientation estimates and equivalent dipole polarizability estimates used for large and shallow UXO/scrap discrimination are more problematic as they are affected by higher order (non-dipole) terms induced in objects due to source field gradients along the length of the objects. In the case when a large shallow object was found, we collected five measurements spaced 0.5 m along a line traversing the object (i.e. if the object location was at 0.0, measurements were taken at 1.0 m, 0.5 m, 0.0 m, -0.5 m, and -1.0 m) so that system got further away from the object, and hence minimized source gradients, at one or more locations. The measurement that best satisfied the criteria described earlier was used for the object characterization.

For some objects in the GPO area we used the cued mode. In this case BUD was brought to marked locations and ran in the discrimination mode. The three discriminating polarizability responses were recorded and visually presented on the computer screen. The depth and horizontal location with respect to the cart was recorded, together with a GPS location of the reference point on the cart. As described earlier, for large shallow objects we collected five measurements spaced 0.5 m along a line traversing the object (i.e. if the object location was at

0.0, measurements were taken at 1.0 m, 0.5 m, 0.0 m, -0.5 m, and -1.0 m). The measurement that best satisfied the criteria described earlier was used for the object characterization.

3.2 Period of Operation

The survey was performed between October 1, 2007 and October 17, 2007. The time required for the major activities involved in the field demonstration are provided in Table 1.

TABLE 1. TOTAL TIME OF MAJOR DEMONSTRATION ACTIVITIES

Task	Time	Notes
Site Orientation, Safety Briefing	3 hr	
Unloading and packing	1 day	½ day unloading, ½ packing
GPS Base Setup	6 hr	30 min/day
Field Checks & Calibrations	12 hr	1 hr/day system and background calibration
GPO	2 days	1 acre
Detection and Discrimination Survey	9.5 days	5 acres
Data Processing, Quality Assurance &Archiving	15 days	
Contingencies	2.5 days	background response variations, repeat measurements, weather related issues, system malfunction
Total Time	15 days	

The following GPS coordinates of our base station were used for BUD positioning: (Easting, Northing) = (509576.94, 4558840.20).

Demobilization consisted of disassembly and removal of the system and packing of the container which took about 3 hours. BUD and all materials and supplies were removed from the site and shipped in the container back to Berkeley, California after the survey.

4. DATA ANALYSIS AND INTERPRETATION

The first step prior to data collection was a system calibration and a background level estimation. We measured the background field on all channels at a place free of metallic objects. This step was repeated at least twice to make sure the background field was stable and could be used as the baseline measurement that was subtracted from the data. The next step was to take data over the calibration target buried in the ground.

Twelve channels of field data are recorded at a rate of 250 k-samples/second for each of three transmitters. Field data were stacked together in a field programmable gate array (FPGA) and transferred to a field computer (laptop) forming a primitive stack, labeled with header information (instrument position, tilt and heading, odometer, time stamp, channels of transmitter

current, etc). An even number of primitive stacks was averaged together to form stacked data for further processing.

The peak transmitter current was estimated from the stacked transmitter current channel record, and the data were normalized by that value. Nominal transmitter shut-off time was estimated, and induction responses were computed at 34 logarithmically spaced times between 140 and 1400 μs, averaged in half-sine windows with widths 10% of the center time after transmitter pulse shut-off. Responses were differenced with background responses collected over a nearby site determined to be relatively free of metallic objects by having a system response which varies little with system translation. Error bars were computed for these based on the scatter in raw 4 μs samples at late time, and used to estimate uncertainties in field inversions of equivalent dipole polarizability responses and object position.

In post processing, the data were reprocessed, with the background response for each line of data computed using a trimmed median response at each time and receiver, for each transmitter response. The trimmed median used is the median of all points within 2 median absolute deviations (MAD) of the (untrimmed) median response at each time, receiver, and transmitter. As the background variation is a larger source of uncertainty than the previously mentioned noise estimated from scatter in raw 4 μs, 1.48 times the MAD in individual line responses were used as the estimated noise level in later processing. The resulting 24 channels of normalized responses were then inverted for candidate object position and principal polarizabilities as a function of time after transmitter shut-off. Data before 140 μs were ignored.

In the half of the GPO surveyed in the detection mode (Figure 8) all the emplaced targets were detected. The color represents the strength of the measured response normalized by the background variation. The detection threshold was set to 7, therefore the red color represent the background response, while yellow, green and blue colors indicate locations of metallic objects. The rest of the GPO area was done in the cued mode due to weather and time constrains. Black symbols indicate locations of stationary BUD measurements, and purple diamonds indicate GPO corners. When a detected object was large/close to the system several measurements were taken as described in Chapter 2.1. The GPO area contains seven different types of UXO – 37 mm projectile, hand grenade, 60 mm mortar, 3" stokes mortar, 75 mm projectile, 81 mm mortar, and 2.36" rocket. Principal polarizability curves as a function of time for these UXO are shown in Figures 9-15.

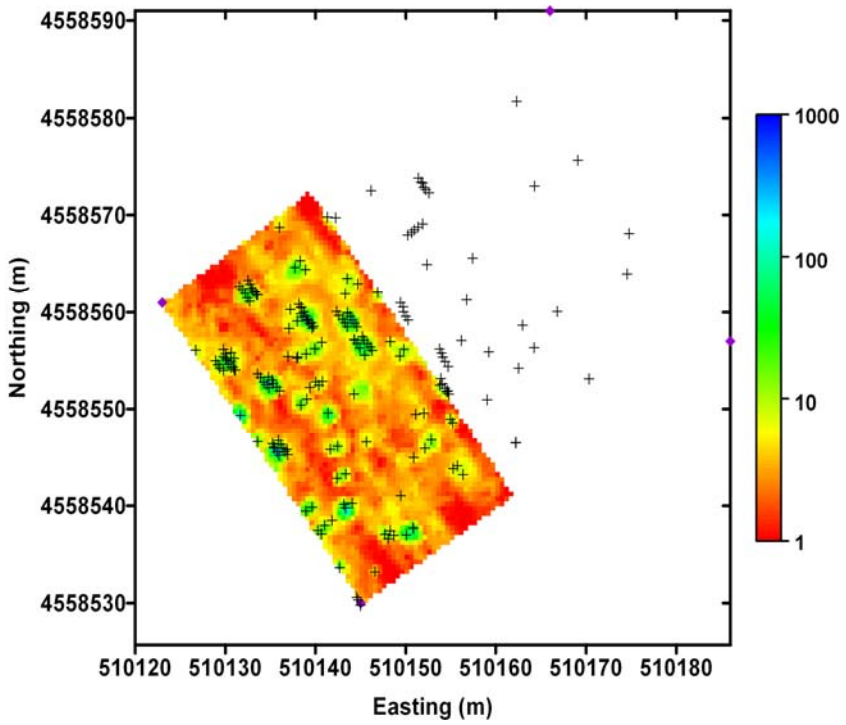

Figure 8. BUD GPO detection map.

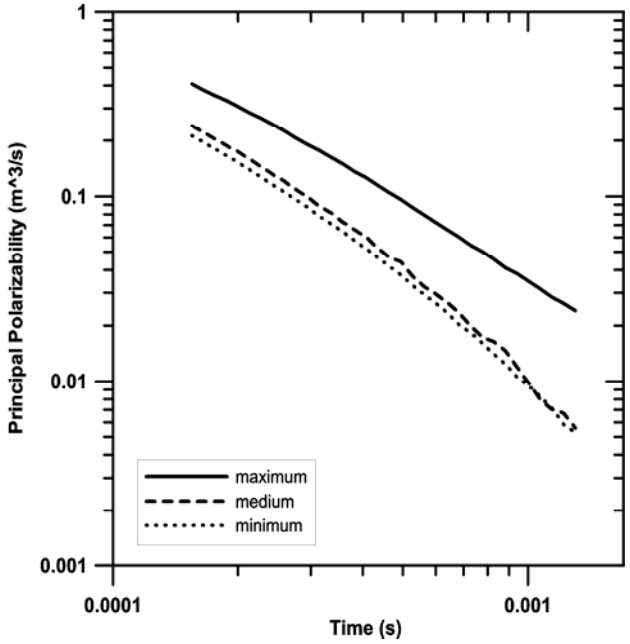

Figure 9. Principal polarizability curves as a function of time for 37 mm projectile.

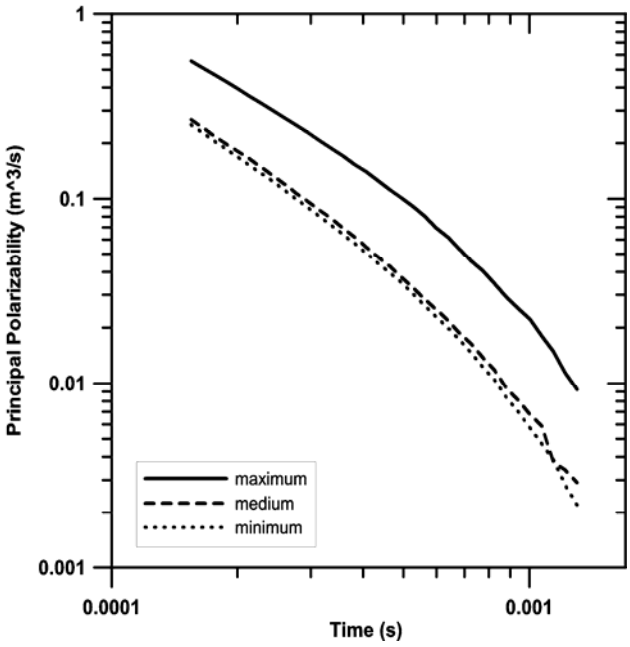

Figure 10. Principal polarizability curves as a function of time for a hand grenade, MK II.

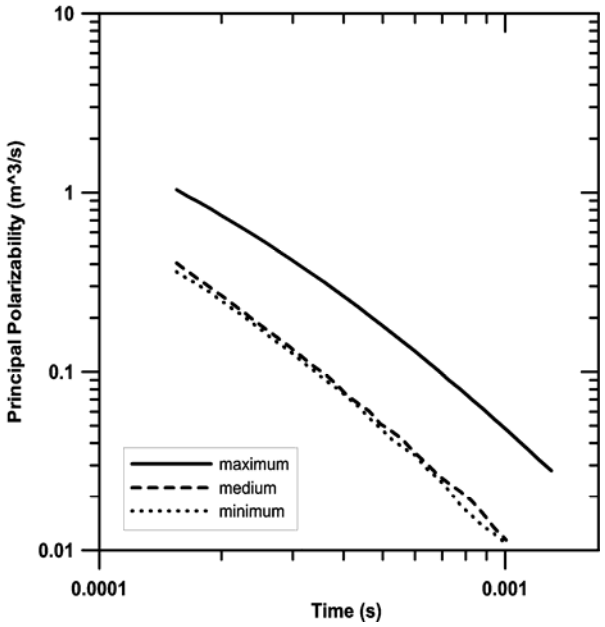

Figure 11. Principal polarizability curves as a function of time for 60 mm mortar.

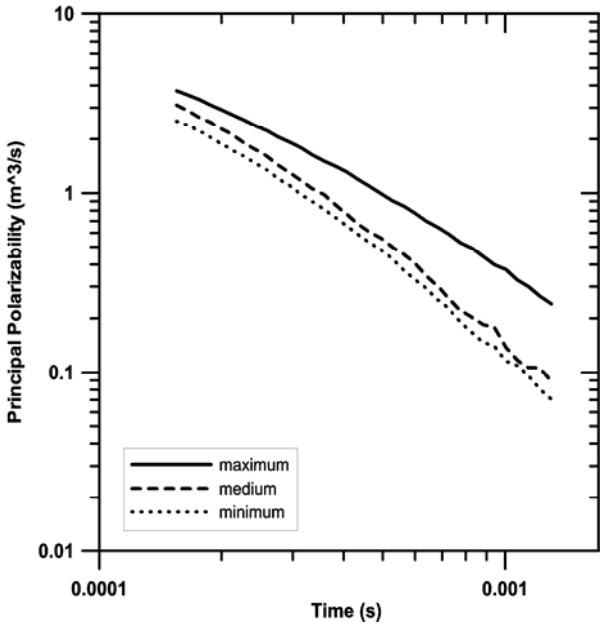

Figure 12. Principal polarizability curves as a function of time for 3” stokes mortar.

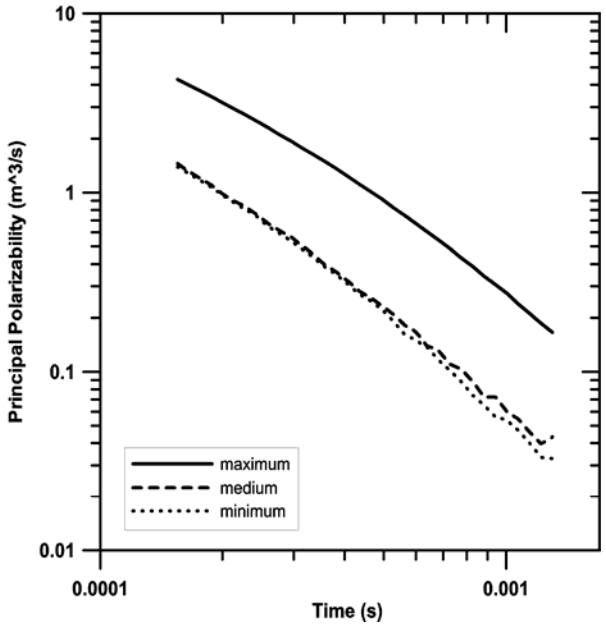

Figure 13. Principal polarizability curves as a function of time for 75 mm AP projectile.

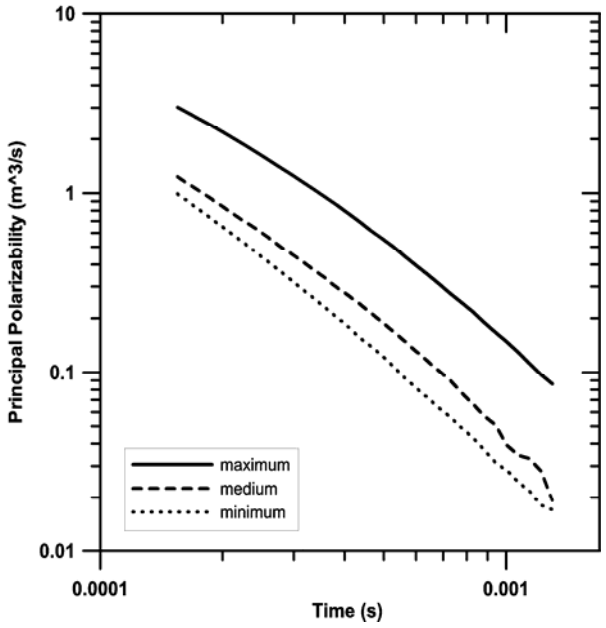

Figure 14. Principal polarizability curves as a function of time for 81 mm mortar.

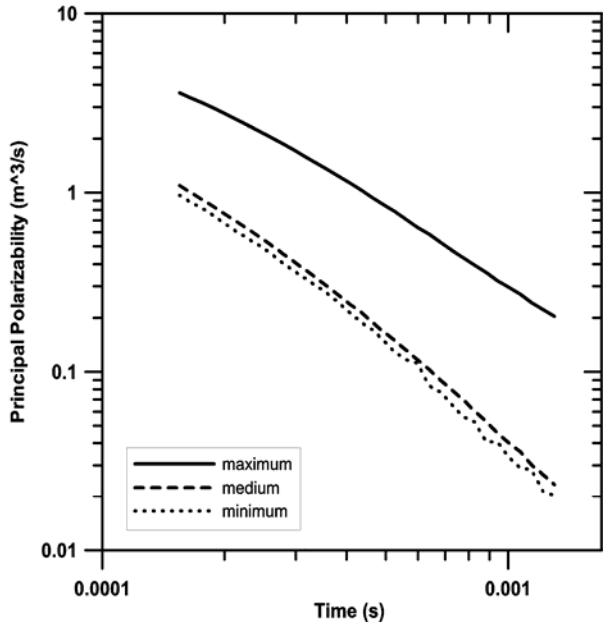

Figure 15. Principal polarizability curves as a function of time for 2.36" rocket.

In our mode of operation several soundings at different locations, are responses of the same object. The discrimination algorithm is based on a single sounding; hence a tool for selecting one sounding per object was required. We developed a means of selecting the most representative sounding from sets of soundings interrogating the same object based on maximum likelihood and using an assumption of Cauchy distributions of the object principal polarizabilities and of their major polarizability axis' dip angle. Our analysis of soundings from the GPO area shows that for 32 soundings when the field strength (the measured signal normalized by Yuma background variations) was greater than 15, the polarizability curves were consistent with axially symmetric objects such as UXO. In the case that this field strength was between 11 and 15, three soundings were consistent (60%) and two were not. The soundings with the field strength below 11 were inconsistent with the response of axially symmetric objects, most likely due to bias in those responses. As we described earlier, we re-processed data

using the GPO MADs instead of Yuma background variations, therefore we calculated the equivalent field strength numbers for 11 and 15, and they were 5.9 and 9.2. The total number of objects in the GPO was 54. We selected 35 soundings consistent with axially symmetric objects responses as UXO training data for use in the discrimination at the Priority 1 survey area. The training data set was expanded by 12 responses of 37 mm, 2.75" and 81 mm UXO acquired in our local test facility, and 16 responses of 2.75", 81 mm and 105 mm UXO from the Yuma Calibration Grid. 179 scrap responses from our survey in Camp Sibert, AL comprised the complimentary scrap training data needed for discrimination. An example of a scrap response is shown in Figure 16.

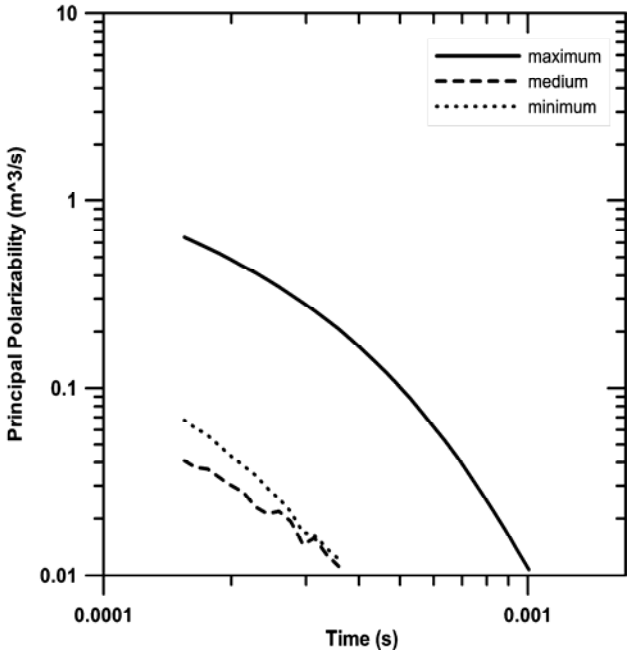

Figure 16. Principal polarizability curves as a function of time for scrap metal.

The Priority 1 area was surveyed in our preferred mode of operation – detection and discrimination at the same time (see Chapter 3.1 for a description of our survey procedure). Figure 17 shows the detection map of this area. Again, the detection threshold was set to 7, therefore red and yellow colors represent the background response, while green and blue colors indicate locations of metallic objects.

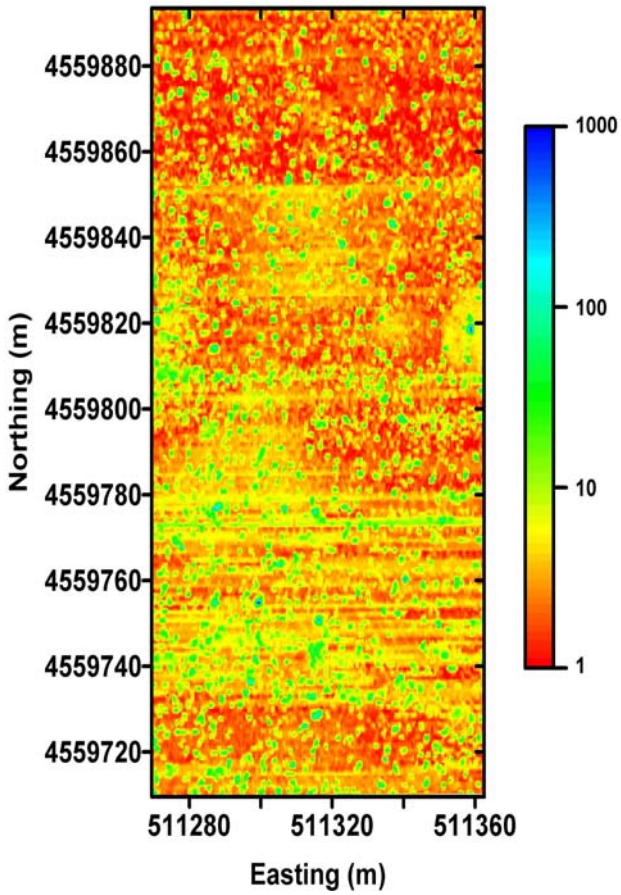

Figure 17. BUD detection map of the Priority 1 area.

In a part of the Priority 1 area (lines 114 – 161, Northing 4559779 – 4559732) we observed a large background response drift in two BUD receiver channels. This was mitigated by implementing inverse weighting by MADS from these lines as a better means of locating

metallic objects in the presence of a large background response. Due to variability of the S/N in data from the Priority 1 area, we calculated field strengths in three different ways – (a) using Yuma background variations, (b) using 1.48 times FE Warren GPO MADs, and (c) using 1.48 times Priority 1 area MADs of lines 114-161. In case (a) we identified 1911 anomalies, 805 of which were above the detection threshold of 7; in case (b) we identified 1873 anomalies, 709 of which were above the detection threshold of 3.5; and in case (c) we identified 1857 anomalies, 783 of which were above the detection threshold of 1.9. Our final interpretation contains a combination of these estimates. For lines 0-113 and 162-184 we used local maxima from a set calculated using option (b), hence any anomaly with a response large then 3.5 was considered to be due to a metallic object. For lines 114-161 we used local maxima from a set calculated using option (c), and therefore any anomaly with response 1.9 or larger was considered to be due to a metallic object. Combining these two data sets resulted in a total of 1533 detected anomalies. Since the data acquired in the discrimination (stationary) mode have higher S/N, we selected those soundings any times when they were nearest to each of the 1533 detected anomalies. In the case when a local maximum (detected anomaly) didn't have a stationary sounding nearby, we used data from the search mode. There were 158 such soundings in our data set.

The Priority 1 area discrimination set contained 1533 detected anomalies. The corresponding polarizability inversion responses were classified as single UXO/not single UXO (e.g., scrap, scrap + UXO, or multiple UXO) using the selected training data (see Appendix A for more details). Figure 18 shows by colors a probability that an identified metallic object is a single UXO. Values are given in fractions, i.e. 1=100%, 0.1=10%. 73 objects (5%) have probability

higher than 50% of being single UXO, 1417 objects (92%) have probability less than 10% of being single UXO, and 728 objects (86%) have probability less than 1% of being single UXO. For the classifications made using most of the training data (but not the low amplitude GPO area object responses), there were 786 maxima with the field strength larger than 9.2, of which 25 (± 2) were estimated to be single UXO, based on the sums of their estimated probabilities of being single UXO and their squares, a 3% positive rate. Based on the comparison of estimated and true depths of UXO in the GPO area, the estimated depths are accurate to ~0.25 m. Of the 747 maxima, with the field strength between below 9.2, 53 (± 3) single UXO are estimated to be present, with an overall total of 78 (± 5) single UXO. For responses with the field strength less than 9.2, assuming a 40% rate of polarizabilities being poorly estimated for accurate identification, and the 3% positive rate among those, suggest a missed identification rate of 1.4%. So, for the objects with low amplitude responses a floor of probability of being UXO was artificially imposed. We place little confidence in the estimated depths of those objects. Despite the fairly low estimated numbers of intact single UXO, to have less than 1% probability of leaving any UXO behind, 835 anomalies need to be dug based on the analyzed data. If that probability would be 10%, 808 anomalies need to be excavated. Figure 19 is a 'priority dig map' where in green we show locations identified as scrap therefore safe to leave in the ground while in red we show locations that need to be dug. We also considered discrimination based on only the selected 35 responses from the GPO area and a subset of 41 scrap responses used as training data in our Camp Sibert discriminations. The third discrimination we considered was based on the largest training data set that included those 19 GPO responses with low amplitude that were excluded from previous training data sets.

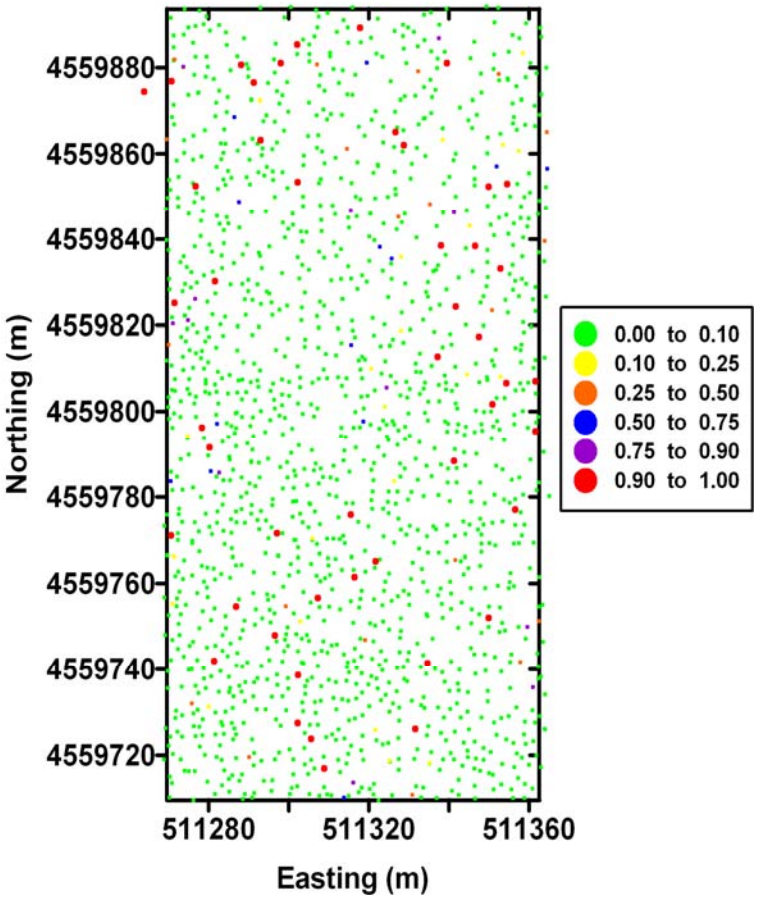

Figure 18. Probability of a metallic object being a single UXO. Values are given in fractions (1=100%, 0.1=10%)

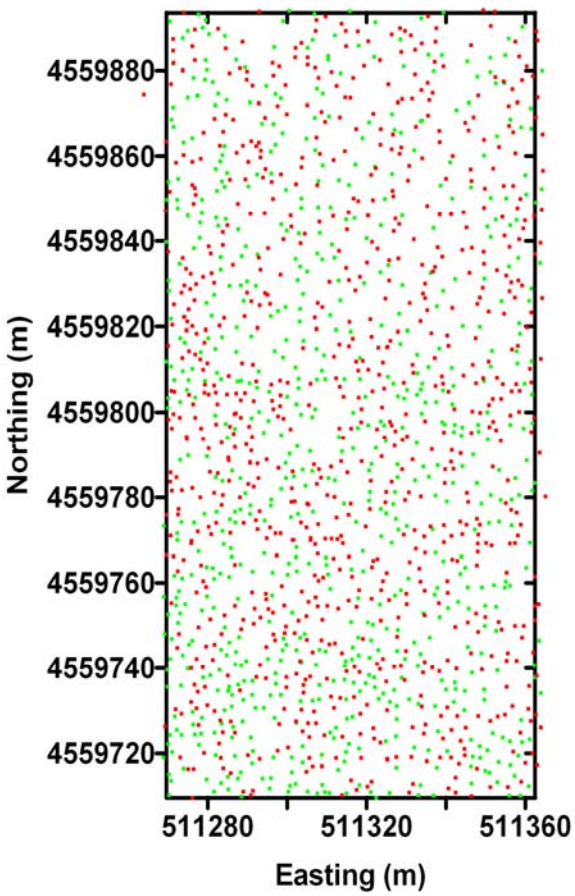

Figure 19. Priority dig map –green dots are identified as scrap while red dots are locations that need to be dug.

5. PERFORMANCE ASSESSMENT

We provide target characteristics (location, size, and polarizability) for detected objects as follows:

(a) x, y, z (depth below the surface) location of object

(b) principal polarizability responses vs. time (as in Figures 2-4)

(c) identification as intact UXO or not single UXO (e.g. scrap, scrap+UXO, multiple UXO)

The priority dig list contains 1533 anomalies that we identified in the Priority 1 area. We estimated that 78 +- 5 single UXO are present. Despite the fairly low estimated numbers of intact single UXO, many objects have low amplitude responses, and hence in order to have less than 1% probability of leaving any UXO behind 835 anomalies need to be dug based on the analyzed data. If that probability would be 10%, 808 anomalies need to be excavated.

Estimation of Receiver Operating Characteristic (ROC) Curves

This section describes how we estimated ROC curves without knowing the ground truth. Given a set of objects with probability p of being UXO and a threshold p_0 for considering object with $p \geq p_0$ to be identified as UXO, if $p \geq p_0$ then all are considered UXO. However, on average a fraction (1-p) of them were not actually UXO, so they were false alarms. If $p_0 > p$ then all are considered non-UXO (scrap), but on average a fraction p of them were actually UXO, so these are missed identifications. Extending this to a set of m objects with probabilities p_i, i=1, m of being UXO, the expected overall false alarm rate is

$$\frac{1}{m}\sum_{p \geq p_0} 1 - p_i \qquad (1)$$

and the expected overall false negative rate is

$$\frac{1}{m}\sum_{p < p_0} p_i \qquad (2)$$

where these rates are per total number of targets. Given the same set of identification probabilities, the expected number of UXO is

$$\sum_i p_i \pm \sqrt{\sum_i p_i - p_i^2}\,, \tag{3a}$$

and of non-UXO is

$$\sum_i 1 - p_i \pm \sqrt{\sum_i p_i - p_i^2} \tag{3b}$$

where the uncertainties are given by the square root of the sum of the variances of the m terms in the sums, and are the same for the two sums. Using these to renormalize Eqs. (1) and (2), the expected false alarm rate per non-UXO is

$$\frac{\sum_{p_i \geq p_0} 1 - p_i}{\sum_i 1 - p_i}, \tag{4}$$

and the expected false negative rate per UXO is

$$\frac{\sum_{p_i < p_0} p_i}{\sum_i p_i}. \tag{5}$$

The ROC curve for the identification problem described above is given in Figure 20.

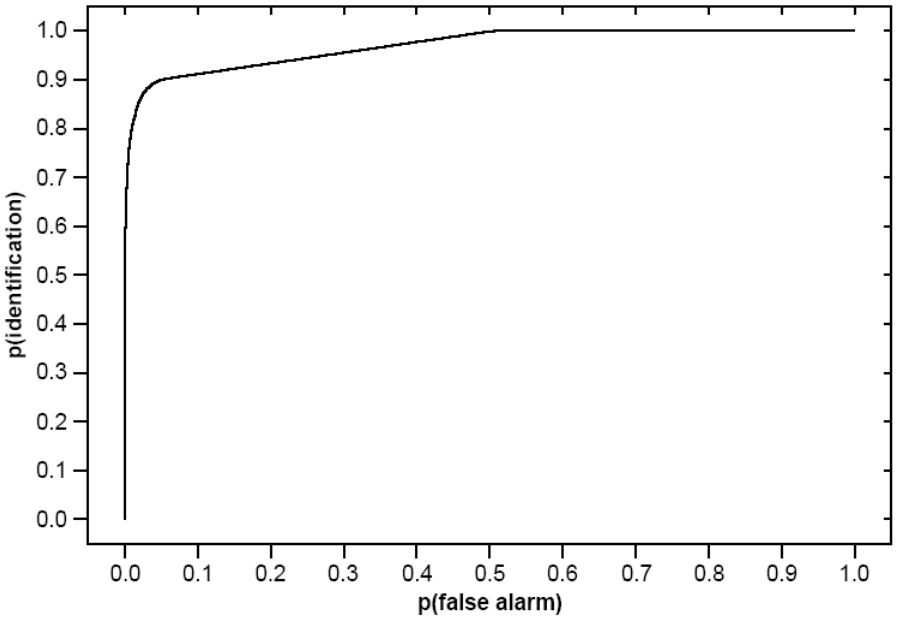

Figure 20: Estimated ROC curve for the targets priority dig list.

6. COST ASSESSMENT

Our preferred mode of operation involves detection and characterization/discrimination at the same time. The advantage of this mode of operation is that target reacquisition is not necessary for discrimination. Hence, this eliminates surveying costs and a second, cued, survey at the expense of smaller daily coverage. We demonstrated this mode of operation in the Priority 1 area. It took us 9.5 days to cover the area (~0.5 acres/day) and 2 days to measure responses in the GPO area. The field crew consisted of two people.

7. REFERENCES

Becker, A., Gasperikova, E., Morrison, H.F., Smith, J.T., 2002, Configuring the AEM System: Partners in Environmental Technology Technical Symposium and Workshop, Washington D.C.

Gasperikova, E., 2003, A new-generation EM system for the detection and classification of buried metallic objects: SEG Expanded Abstracts, pp. 2379-2382.

Gasperikova, E., Becker, A., Morrison, H.F., Smith, J.T., 2003, EM sensors for detection and characterization of buried metallic objects: Partners in Environmental Technology Technical Symposium and Workshop, Washington D.C., p. 36.

Gasperikova, E., Becker, A., Morrison, H.F., Smith, J.T., 2005, A multisensor system for the detection and characterization of UXO: SAGEEP, Atlanta.

Gasperikova, E., Smith, J.T., Morrison, H.F., Becker, A., 2006, UXO detection and characterization using new Berkeley UXO Discriminator (BUD): Joint Assembly, Baltimore.

Gasperikova, E., Smith, J.T., Morrison, H.F., Becker, A., 2006, Berkeley UXO Discriminator (BUD) for UXO Detection and Discrimination: Partners in Environmental Technology Technical Symposium and Workshop, Washington D.C.

Gasperikova, E., Smith, J.T., Morrison, H.F., Becker, A., 2007, Berkeley UXO Discriminator (BUD): SAGEEP, Denver.

Gasperikova, E., Smith, J.T., Morrison, H.F., Becker, A., 2007, UXO Detection and Discrimination with Berkeley UXO Discriminator (BUD): UXO Forum, Orlando, FL.

Gasperikova, E., Smith, J.T., Morrison, H.F., Becker, A., 2007, Berkeley UXO Discriminator (BUD) at Camp Sibert, AL: Partners in Environmental Technology Technical Symposium and Workshop, Washington D.C.

Morrison, H.F., 2004, A Multisensor System for the Detection and Characterization of UXO, ESTCP Proposal UX-0437.

Morrison, H.F., Becker, A., Gasperikova, E., Smith, J.T., 2004, A multisensor system for the detection and characterization of UXO: Partners in Environmental Technology Technical Symposium and Workshop, Washington D.C.

Morrison, H.F., Smith, J.T., Becker, A., Gasperikova, E., 2005, Detection and Classification of Buried Metallic Objects, SERDP UX-1225 Final Report.

Smith, J.T., and Morrison, H.F., 2004, Estimating equivalent dipole polarizabilities for the inductive response of isolated conductive bodies: IEEE Trans. Geosci. Remote Sensing, **42**, p. 1208-1214.

Smith, J.T., and Morrison, H.F., Becker, A., 2004a, Parametric forms and the inductive response of a permeable conducting sphere: Journal of Env. And Engin. Geophysics, **9**, p. 213-216.

Smith, J.T., and Morrison, H.F., Becker, A., 2004b, Resolution depths for some transmitter-receiver configurations: IEEE Trans. Geosci. Remote Sensing, **42**, p. 1215-1221.

Smith, J.T., and Morrison, H.F., Becker, A., 2005, Optimizing receiver configurations for resolution of equivalent dipole polarizabilities in situ: IEEE Trans. Geosci. Remote Sensing, **43**, p. 1490 - 1498.

Smith, J.T., and Morrison, H.F., 2006, Approximating spheroid inductive responses using spheres: Geophysics, **71**, p. G21-G25.

Smith, J.T., Morrison, H.F., Doolittle, L.R., and Tseng, H-W., 2007, Multi-transmitter null coupled systems for inductive detection and characterization of metallic objects: Journal of Applied Geophysics, **61**, p. 227–234

APPENDIX A.

UXO DISCRIMINATION USING TRAINING DATA

Training data consisted of a set of principal polarizability responses at 34 logarithmically spaced times centered from 140 μs to 1400 μs after transmitter shut-off. This data set consisted of 35 UXO from the GPO area, 12 responses of 37 mm, 2.75" and 81 mm UXO acquired in our local test facility, 16 responses of 2.75", 81 mm and 105 mm UXO from the YPG Calibration Grid, and 179 scrap responses from our survey in Camp Sibert, AL. Discrimination was made for UXO vs. scrap responses.

The data time interval was sub-divided logarithmically into a number n_{div} of sub-intervals (e.g., 6). The product of each principal polarizability with its sample time was averaged over each of these intervals. Since there are three principal polarizabilities, this results in $n_{feat} = 3n_{div}$ reduced data, hence forth called 'features'. Additional feature used in the analysis was a median $\log_e$(magnitude) (in m^3) which increased the total number of features n_{feat} to $3n_{div}$ +1. The number of sub-divisions n_{div} was chosen using cross validation. In cross validation, an analysis method is applied to most of a training data set and the results are used to predict something about the remaining (excluded) training data. This is done many times, excluding a different set of training data each time, and a choice made, e.g., the value of n_{div}, based on what gives the best predictions averaged over many times.

In our application, two thirds of the training data were randomly selected for direct use in training, and one third was reserved for later calibration and is termed 'reserved data'. Based on the selected 2/3 of the training data, the probability that an observation is due to scrap is estimated from a ratio of empirical probability density estimates for feature values. Empirical probability distributions are probability distribution estimates made based on observed data. Empirical probability distributions will be constructed below.

Within the selected 2/3 of the training data ('non-reserved' data), additional responses were randomly selected for exclusion in cross validation, and are termed 'excluded data'. In this work, a constant number of UXO training data, and a constant number of scrap training data were excluded at a time, in roughly equal proportions. The number of excluded data was chosen so that one response was withheld at a time from the smaller of the sets of non-reserved UXO and scrap training data. In cross validation one UXO and one scrap were withheld from the training responses at a time. This was cycled through all excluded responses excluding each scrap and each UXO responses once.

We estimate empirical probability densities separately for UXO and scrap classes. In constructing an empirical probability distribution for either UXO or scrap responses, it is desirable to smear probability associated with any particular data point into a region centered around it, as it is extremely unlikely that another data point will have exactly that value. To get an idea of how much to smear out the probability associated with each data point in forming an

empirical probability distribution, a trimmed cross power matrix is constructed for variation of data vectors about their median values. To do this, within training data for a class, values of each feature are sorted, the median and median absolute deviation (MAD) from the median are noted. In finding these medians and MADs, responses reserved for calibration and responses excluded for cross-validation are omitted. The values for each feature are then shifted by subtracting its median value. As the scale of different features may vary from feature to feature, before forming the trimmed cross power matrix, the shifted feature values for each feature are normalized by dividing their MAD resulting in shifted normalized feature vectors, $\mathbf{v}_i^{(UXO)}$ for UXO responses, and $\mathbf{v}_i^{(scrap)}$ for scrap responses. Trimmed cross power matrices $\mathbf{C}^{(class)}$ are computed from these, with superscript $^{(class)}$ meaning either $^{(uxo)}$ or $^{(scrap)}$. To compute the trimmed cross power matrix for a class, values of $|\mathbf{v}_i^{(scrap)}|$ are computed for the class's training data and sorted to find median($|\mathbf{v}_i^{(scrap)}|$), omitting reserved and excluded data. Then the class trimmed cross power matrices are computed as

$$C^{(class)} = \frac{1}{\tilde{n}^{(class)}}\left[\sum_{i \text{ in class}, \left|v_i^{(class)}\right| \le \text{median}} v_i^{(class)} \left(v_i^{(class)}\right)^t + \sum_{i \text{ in class}, \left|v_i^{(class)}\right| > \text{median}} \text{median}^2 \frac{v_i^{(class)} \left(v_i^{(class)}\right)^t}{\left|v_i^{(class)}\right|^2}\right] \qquad (A.1)$$

where $\tilde{n}^{(class)} \equiv n^{(class)} - n^{(class)}_{rsrv} - n^{(class)}_{with}$, and $n^{(class)}_{rsrv}$, is the number of (class) responses reserved for subsequent calibration, and $n^{(class)}_{with}$ is the number of (class) responses excluded as a part of cross validation. The sums are over all non-excluded non-reserved class responses, t denotes transpose, and median means median($|\mathbf{v}_i^{(scrap)}|$). In the second sum, the contribution of

large magnitude feature vectors are downweighted. Feature vector $\mathbf{v}_i^{(\text{class})}$ probability density function is estimated empirically as proportional to

$$f^{(\text{class})}(v_j^{(\text{class})}) = K \sum_{i \text{ in class}} \frac{1}{\left[1 + (v_j - v_i)^t (C^{(\text{class})})^{-1} (v_j - v_i)(\tilde{n}^{(\text{class})})^{-1/2n_{\text{feat}}}\right]^{(3+n_{\text{feat}})/2}} \tag{A.2}$$

with

$$1/K = (\tilde{n}^{(\text{class})})^{(1+n_{\text{feat}})/n_{\text{feat}}} (\det(C^{(\text{class})}))^{1/2} \tag{A.3}$$

where superscript $^{(\text{class})}$ has been omitted from $\mathbf{v}_i^{(\text{class})}$ and $\mathbf{v}_j^{(\text{class})}$ in the denominator, and reserved and excluded $\mathbf{v}_i^{(\text{class})}$ terms omitted from the sum. Quantity in Eq. A.2 will be referred to as a density, although strictly speaking a density is normalized to have unit integral, and quantity in Eq. A.2 has not been normalized. Eq. A.2 is a generalization of a Cauchy distribution, with the outer exponent being the smallest half integer value yielding a finite variance.

In cross validation, densities (Eq. A.2) are computed for UXO and scrap classes from non-excluded responses, and feature vectors $\mathbf{v}_j^{(\text{uxo})}$ and $\mathbf{v}_j^{(\text{scrap})}$ are computed for excluded training responses not reserved for calibration, where for the j'th response, the two differ in component offsets and normalizations. The first is used in estimating the response's likelihood as a UXO response, and the second in estimating its likelihood as a scrap response. For a given response, assuming that the proportionality constant is the same for both UXO and scrap estimated densities, the probability that the response is due to a scrap would be

$$\frac{f^{(\text{scrap})}(v_j^{(\text{scrap})})}{f^{(\text{uxo})}(v_j^{(\text{uxo})}) + f^{(\text{scrap})}(v_j^{(\text{scrap})})} \tag{A.4}$$

as the common proportionality factor cancels in their ratio. The probability that is due to UXO, would be one less this number. Allowing for a ratio of proportionality constants to be α^2, the densities are then $\alpha f^{(uxo)}(\mathbf{v}_j^{(uxo)})$ and $f^{(scrap)}(\mathbf{v}_j^{(scrap)})/\alpha$ (within a common scale factor), and the probability that the response is due to scrap is

$$p^{(scrap)}(v_j^{(scrap)}) = \frac{f^{(scrap)}(v_j^{(scrap)})}{\alpha^2 f^{(uxo)}(v_j^{(uxo)}) + f^{(scrap)}(v_j^{(scrap)})} \tag{A.5}$$

and the UXO probability its compliment $(1 - p^{(scrap)})$. The probability in Eq. A.5 depends only on α^2, $f^{(uxo)}(v_j^{(uxo)})$, and $f^{(scrap)}(v_j^{(scrap)})$. The latter two are computed and saved for each excluded training datum, and proportionality constant α^2 chosen subsequently.

In short, after computing $f^{(scrap)}(\mathbf{v}_j^{(scrap)})$ and $f^{(uxo)}(\mathbf{v}_j^{(uxo)})$ for the set of excluded responses not reserved for calibration, the set of excluded responses is changed, trimmed feature covariance matrices recomputed, and densities computed for the set of new unreserved excluded responses. Again, $n^{(scrap)}_{with}$ is the number of scrap training data withheld as a part of cross validation in each cycle, $n^{(uxo)}_{with}$ is the similar number of UXO training data withheld in each cycle. Letting n_{cycl} be the number of cycles of excluding some training data, $n_{cycl} \times n^{(scrap)}_{with}$ unreserved scrap training responses, and $n_{cycl} \times n^{(uxo)}_{with}$ unreserved UXO training responses are cycled through the excluded set. For a given value of α^2, the scrap probabilities associated with these values are summed as

$$\left\langle \tilde{n}^{(scrap)} \right\rangle = \sum_{j \text{ exluded, not reserved}} p^{(scrap)}(v_j^{(scrap)}) \tag{A.6}$$

Since the number of scrap responses that have been thus excluded is known to be $n_{cycl} \times n^{(scrap)}_{with}$, parameter α^2 is adjusted, so that

$$<\tilde{n}^{(scrap)}> = n_{cycl} \times n^{(scrap)}_{with} \quad (A.7)$$

Eq. A.6 is monotonic in α^2, so solution is unique. Newton's method started from $\alpha^2 = 1$, keeping α^2 from decreasing to less than 0.1 of its previous value on any iteration, works very well. Since $p^{(scrap)} = 1 - p^{(uxo)}$, the criterion for setting α^2 also sets the sum of $p^{(uxo)}$ ($\mathbf{v}_j^{(uxo)}$) to the number of UXO responses cycled through the excluded training data set $n_{cycl} \times n^{(uxo)}_{with}$.

For a prospective number of sub-intervals n_{div}, cross power matrices $\mathbf{C}^{(class)}$ are 3 n_{div}+1 x 3 n_{div}+1 square matrices requiring at least 3 n_{div}+1 vector outer products to be summed (in Eq. A.1) to avoid singularity. This limits the prospective numbers of time interval sub divisions to

$$n_{div} \leq \min(\tilde{n}^{(scrap)}, \tilde{n}^{(uxo)})/3 \quad (A.8)$$

but sub-divisions near the limiting value are expected to give poor results due to variance in the cross power matrix estimates.

In general UXO identifications are made by choosing a threshold value $p_o^{(uxo)}$ above which responses are considered to be due to UXO. To obtain as few missed identifications as possible for a given level of $p_o^{(uxo)}$, it is desirable to have as few true UXO responses with $p^{(uxo)}$ below this level as possible, that is, as many with $p^{(scrap)} = 1 - p^{(uxo)}$ below $p_o^{(scrap)} = 1 - p_o^{(uxo)}$ as possible. To select a number of interval sub-divisions that will work well with a variety of threshold values, we choose n_{div} minimizing the sum

$$\left\langle \tilde{n}^{(miss)} \right\rangle = \sum_{j\,uxo,\,not\,reserved} p^{(scrap)}(v_j^{(scrap)}) \qquad (A.9)$$

If some UXO response looks totally like a scrap response then it would contribute 1 to $<\tilde{n}^{(miss)}>$ in summation in Eq. A.9; if it looks nothing like scrap responses it would contribute 0 to $<\tilde{n}^{(miss)}>$. So, quantity $<\tilde{n}^{(miss)}>$ is a measure of how much the UXO training data look like scrap responses under the classifier (choice of n_{div}) being considered. For each value of n_{div} tried, $<\tilde{n}^{(miss)}>$ is computed using values $p^{(scrap)}$ ($\mathbf{v}_j^{(scrap)}$) which are computed using cross validation.

Recapping, 1/3 of the training data is reserved for later use; the remaining UXO and scrap data are randomly ordered within each of these classes. A sequence of candidate n_{div} values are cycled through an outer loop. Sets of excluded UXO and scrap training data are chosen starting with the first on their randomly ordered lists. Trimmed feature covariance matrices are computed excluding these and the reserved data. Quantities $f^{(scrap)}$ ($\mathbf{v}_j^{(scrap)}$) and $f^{(uxo)}$ ($\mathbf{v}_j^{(uxo)}$) are computed for the excluded data. The sets of excluded responses are changed (moving down the random ordered lists), trimmed feature covariance matrices recomputed, and densities computed for the new set of unreserved excluded responses, based on the non-excluded unreserved responses. After cycling essentially all of the non-reserved training data through the excluded sets, α^2 is chosen (for the current n_{div}) using Newton's method to enforce criterion in Eq. A.7. That is, the sum of scrap probabilities over responses that have been, in turn, excluded from the covariance matrix sums (Eq. A.1) and the empirical density sum (Eq. A.2), is equal to the number of scrap responses among these. Then, with this value of α^2, the sum of estimated scrap probabilities over the UXO responses that have been in turn excluded, is computed (Eq. A.9).

This whole sequence is repeated for each candidate value of n_{div}, and n_{div} giving the lowest value of Eq. A.9 is selected.

Once n_{div} has been selected, covariance matrices $C^{(uxo)}$ and $C^{(scrap)}$ are recomputed using all non-reserved training data to compute feature medians and MADs for UXO and for scrap responses, and in forming the covariance matrices themselves. Similarly, all non-reserved training data are then used in reforming empirical distributions for scrap and UXO classes analogously to Eqs. A.2 and A.3 but summed over all the non-reserved responses, omitting any self-response terms (i=j), with the numbers of non-reserved UXO and scrap responses $\tilde{n}^{(uxo)}$ and $\tilde{n}^{(scrap)}$, replacing $\tilde{n}^{(class)}$ appropriately. Then all data, reserved and non-reserved, is used in computing an estimated number of scrap responses $<n^{(scrap)}>$ analogously to Eq. A.6, and α^2 reselected, so that the resulting $<n^{(scrap)}>$ is equal to the total number of scrap responses, to calibrate the resulting empirical distributions and probabilities. In this step, the inclusion of non-reserved data (which entered into the covariance matrices) in the probability sums used in the final calibration, may bias the resulting probabilities somewhat, but is thought to be more than compensated for in reduced variance in the final value of α^2 obtained. The inclusion of the 1/3 of reserved data, that was omitted in estimation of the feature covariance matrices, in the probability sum $<n^{(scrap)}>$ used in the final calibration, lessens the effect of any such bias.

The resulting covariance estimates, empirical probability distributions for v^{scrap} and v^{uxo} and proportionality constant α^2 are then used to evaluate the probability that a response is due to

scrap through Eq. A.5 evaluated using the response's feature vector, shifted and normalized as a prospective scrap response v^{scrap} and as a prospective UXO response v^{uxo}.